

Fast Computation of 3D Spherical Fourier Harmonic Descriptors - A Complete Orthonormal Basis for a Rotational Invariant Representation of Three-Dimensional Objects

Henrik Skibbe

Qing Wang, Olaf Ronneberger, Hans Burkhardt
Department of Computer Science
Center for Biological Signalling Studies (bloss)
Albert-Ludwigs-Universität Freiburg, Germany

skibbe@informatik.uni-freiburg.de

Marco Reisert

Dept. of Diagnostic Radiology, Medical Physics
University Medical Center, Freiburg

marco.reisert@uniklinik-freiburg.de

Abstract

In this paper we propose to extend the well known spherical harmonic descriptors[6] (SHD) by adding an additional Fourier-like radial expansion to represent volumetric data. Having created an orthonormal basis on the ball with all the gentle properties known from the spherical harmonics theory and Fourier theory, we are able to compute efficiently a multi-scale representation of 3D objects that leads to highly discriminative rotation-invariant features, which will be called spherical Fourier harmonic descriptors (SFHD). Experiments on the challenging Princeton Shape Benchmark (PSB[16]) demonstrate the superiority of SFHD over the ordinary SHD.

1. Introduction

With the increasing performance of modern computer systems the number of volumetric images derived from stereo vision systems, laser scanning devices or microscopical recordings has drastically increased in recent years. In many applications three-dimensional objects must be described and classified in a space- and time-saving manner. These descriptions should be robust or invariant to certain transformations, and discriminative. One possible solution are object descriptors which rely on the idea of group integration, where certain features are averaged over the whole group to become invariant [15, 9]. For the rotation group the spherical harmonics can directly be utilised to obtain rotation invariant object representations in an analytical way, as shown e.g. in [6, 10, 13]. The major disadvantage of this approach is the restriction to spherical functions. This means, that the spherical harmonic descriptors for three-dimensional scalar fields are based on a function expansion done for an (theoretically) infinite set of nested spheres. Hence, from a practical point of view,

a dense set of nested spheres is necessary to represent an object sufficiently. The descriptors representing different spheres are then invariant to inner object rotations (see [6] for examples.), which in many cases weakens the ability of object discrimination. We can overcome this limitation by using an additional radial expansion as proposed for instance in [7, 17, 2]. Experiments in [17] have already shown that the consideration of a radial expansion increases the performance in object classification tasks. In contrast to [7, 17, 2], we propose a radial expansion which is based on a Fourier-like basis that has already been widely used in a similar way for two-dimensional image representation and feature generation. (Known as angular radial transformation, see e.g. [3, 12]). The transformation for volumetric data which we propose here has some very nice properties: fast algorithms are available for both, the spherical harmonics transformation[8] and the Fourier transformation[4]. We further can make use of the spherical tensor product[11] to preserve the phase information of expansion coefficients in the final object descriptors. The descriptors will be called spherical Fourier harmonic descriptors (SFHD). We conduct experiments on the challenging Princeton Shape Benchmark (PSB[16]) containing 1814 objects by comparing the performance of ordinary SHD to our SFHD leading to very promising results.

The paper is organised in four further sections. Section 2 gives a short introduction to the mathematical definitions and notations we use. In Section 3, we introduce an orthonormal basis system on the ball, which will be utilised to derive rotation invariant descriptors from volumetric image data. Our Experiments are discussed in section 4 and our conclusion is given in section 5.

2. Preliminaries

We assume that the reader has basic knowledge in the theory and notations of the harmonic analysis of $SO(3)$, meaning he or she should have knowledge both in spherical harmonics and in Wigner D-Matrices. The reader should also know how and why we can obtain rotation invariant features from spherical harmonic coefficients [6].

A good start for readers who are completely unfamiliar with the theory might be [5], where a basic understanding of spherical harmonics is given, focused on a practical point of view. The design of rotation invariant spherical harmonic features was first addressed in [6]. Deeper views into the theory are given in [14, 11, 1]. However, we first want to recapitulate the mathematical notations and definitions which we will use in the following sections.

Let \mathbf{D}_g^ℓ be the unitary irreducible representation of a $g \in SO(3)$ of order $\ell \in \mathbb{N}$, acting on the vector space $\mathbb{C}^{2\ell+1}$. They are widely known as Wigner D-Matrices [14]. We denote the complex conjugate of a vector $\mathbf{a} \in \mathbb{C}^n$ by $\bar{\mathbf{a}}$ and the transpose of \mathbf{a} by \mathbf{a}^T . Depending on the context we will express the coordinate vector $\mathbf{r} = (x, y, z)^T \in \mathbb{R}^3$ in spherical coordinates (r, θ, ϕ) , which is closer to the commonly used notation of spherical harmonics, where:

$$r = \|\mathbf{r}\| = \sqrt{x^2 + y^2 + z^2} \quad (1)$$

$$\theta = \arccos\left(\frac{z}{\sqrt{x^2 + y^2 + z^2}}\right) \quad (2)$$

$$\phi = \text{atan2}(y, x) \quad (3)$$

2.1. Spherical Harmonics Basis Functions

In our work we use the following definition of the spherical harmonics:

$$Y_m^\ell(\theta, \phi) = \sqrt{\frac{2\ell+1}{4\pi} \frac{(\ell-m)!}{(\ell+m)!}} P_\ell^m(\cos\theta) e^{im\phi} \quad (4)$$

with $\ell \in \mathbb{N}_0, m \in \mathbb{Z}, |m| \leq \ell$ and associated Legendre functions P_ℓ^m . The functions Y_m^ℓ build a countably infinite complete orthonormal basis for representing functions on the 2-sphere,

$$\begin{aligned} \langle Y_m^\ell, Y_{m'}^{\ell'} \rangle &= \int_0^\pi \int_0^{2\pi} Y_m^\ell(\theta, \phi) \overline{Y_{m'}^{\ell'}(\theta, \phi)} d\Omega \\ &= \delta_{\ell\ell'} \delta_{mm'} \end{aligned} \quad (5)$$

where $\langle \cdot, \cdot \rangle$ denotes the scalar product, $d\Omega = \sin\theta d\phi d\theta$ and δ denotes the Kronecker symbol. A square-integrable

function f on the unit sphere can thus be expanded as:

$$\begin{aligned} f(\theta, \phi) &= \sum_{\ell=0}^{\infty} \sum_{m=-\ell}^{m=\ell} b_{\ell m} Y_m^\ell(\theta, \phi) \\ &= \sum_{\ell=0}^{\infty} (\mathbf{b}_\ell)^T \mathbf{Y}^\ell(\theta, \phi) \end{aligned} \quad (6)$$

with expansion coefficients $\mathbf{b}_\ell \in \mathbb{C}^{2\ell+1}$. A very important property which has been utilised for deriving rotation invariant descriptors in an analytical way from three-dimensional scalar fields [6] is the rotation behaviour of the spherical harmonics expansion coefficients. A rotation $g \in SO(3)$ with corresponding Wigner D-Matrix \mathbf{D}_g acting on a spherical function f transforms the expansion coefficient \mathbf{b}_ℓ to \mathbf{b}'_ℓ with

$$\mathbf{b}'_\ell = \mathbf{D}_g^\ell \mathbf{b}_\ell \quad (7)$$

2.2. 1D Fourier Basis Functions

The Fourier basis

$$w_k^R(r) = \frac{1}{\sqrt{R}} e^{2\pi i k r \frac{1}{R}} \quad (8)$$

is a countably infinite complete orthonormal basis system for functions on the interval $[0, R]$, where $k \in \mathbb{Z}$ and $R \in \mathbb{R}_{>0}$ with

$$\begin{aligned} \langle w_k^R, w_{k'}^R \rangle &= \int_0^R w_k^R(r) \overline{w_{k'}^R(r)} \\ &= \int_0^R w_k^R(r) w_{-k'}^R(r) = \delta_{kk'} \end{aligned} \quad (9)$$

2.3. Spherical Tensor Product

We further need to define the bilinear form $\bullet_0 : \mathbb{C}^{2\ell+1} \times \mathbb{C}^{2\ell'+1} \rightarrow \mathbb{C}$ (a special case of the spherical tensor product [11]) which we use to couple expansion coefficients of equal rank :

$$(\mathbf{u} \bullet_0 \mathbf{v}) := \sum_{m=-\ell}^{m=\ell} (-1)^m u_m v_{-m} \quad (10)$$

with $\mathbf{u}, \mathbf{v} \in \mathbb{C}^{2\ell+1}$. Assume a rotation $g \in SO(3)$ is acting on two expansion coefficients \mathbf{b}_ℓ and \mathbf{b}'_ℓ , where $\mathbf{b}_\ell, \mathbf{b}'_\ell \in \mathbb{C}^{2\ell+1}$. The bilinear form has one very important property: coupling two expansion coefficients preserves the rotation. In our case:

$$\begin{aligned} ((\mathbf{D}_g^\ell \mathbf{b}_\ell) \bullet_0 (\mathbf{D}_g^\ell \mathbf{b}'_\ell)) &= \mathbf{D}_g^0 (\mathbf{b}_\ell \bullet_0 \mathbf{b}'_\ell) \\ &= (\mathbf{b}_\ell \bullet_0 \mathbf{b}'_\ell) \end{aligned} \quad (11)$$

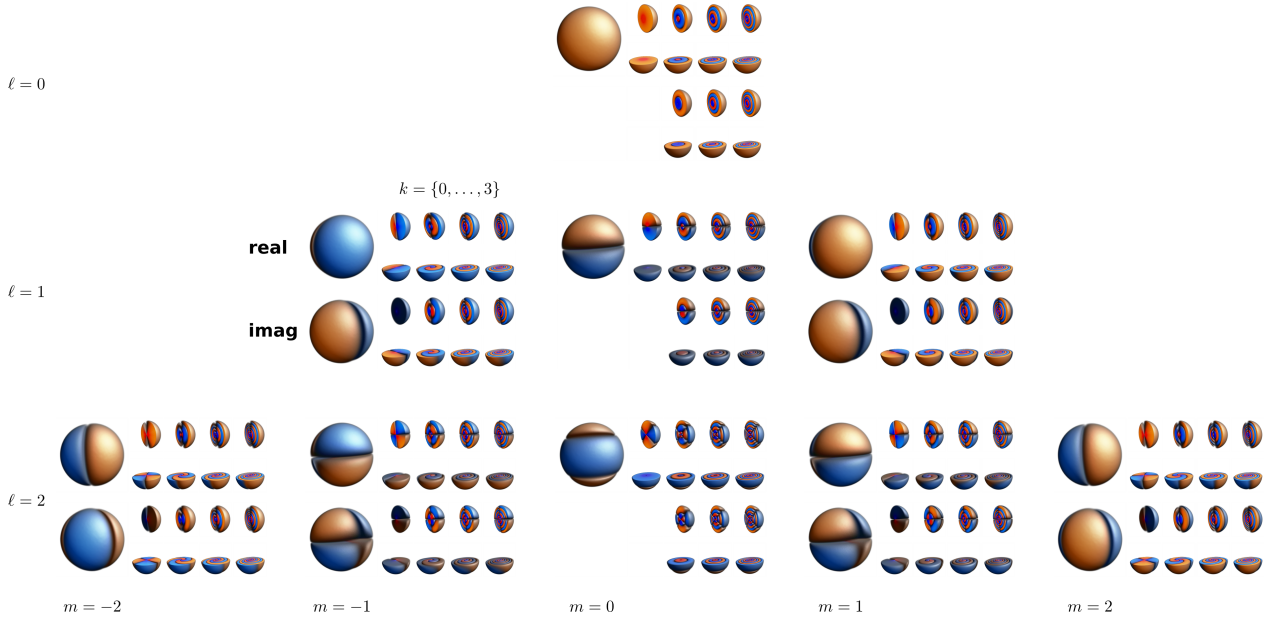


Figure 1. Spherical Fourier harmonics basis functions $E_{\ell m}^{Rk}(\theta, \phi, r) = Y_m^\ell(\theta, \phi)w_k^R(r)\frac{1}{r}$ for $\ell \in \{0 \dots 2\}$ and $k \in \{0 \dots 4\}$. Negative values are depicted in blue, positive values in yellow. The term $\frac{1}{r}$ is indicated by darkening the colour for higher (inner) values.

3. An Orthogonal System on the Closed Ball

We propose to expand a function f which is defined on the ball with given radius $R \in \mathbb{R}_{>0}$ by a set of orthonormal basis functions derived by combining the spherical harmonic expansion describing the angular part, and a damped Fourier expansion describing the radial part. The expansion is given by

$$\begin{aligned} f(\mathbf{r}) &= \sum_{k=-\infty}^{k=\infty} \sum_{\ell=0}^{\ell=\infty} \sum_{m=-\ell}^{m=\ell} a_{\ell m}^{Rk} E_{\ell m}^{Rk}(\mathbf{r}) \\ &= \sum_{k=-\infty}^{k=\infty} \sum_{\ell=0}^{\ell=\infty} (\mathbf{a}_\ell^{Rk})^T \mathbf{E}_\ell^{Rk}(\mathbf{r}) \end{aligned} \quad (12)$$

with expansion coefficients $\mathbf{a}_\ell^{Rk} \in \mathbb{C}^{2\ell+1}$ and orthonormal basis functions

$$E_{\ell m}^{Rk}(\mathbf{r}) = Y_m^\ell(\theta, \phi)w_k^R(r)\frac{1}{r} \quad (13)$$

where

$$\begin{aligned} \langle E_{\ell m}^{Rk}, E_{\ell' m'}^{Rk'} \rangle &= \\ &= \int_0^R \int_0^\pi \int_0^{2\pi} E_{\ell m}^{Rk}(\mathbf{r}) \overline{E_{\ell' m'}^{Rk'}(\mathbf{r})} r^2 d\Omega dr \\ &= \delta_{\ell\ell'} \delta_{mm'} \delta_{kk'} \end{aligned} \quad (14)$$

Given a real-valued function, the coefficients are symmetrically related by

$$a_{\ell m}^{Rk} = (-1)^m \overline{a_{\ell, -m}^{R, -k}} \quad (15)$$

The first 36 basis functions for $\ell \in \{0 \dots 2\}$ and $k \in \{0 \dots 4\}$ are depicted in figure 1.

3.1. Fast Computation of Expansion Coefficients

The computation of expansion coefficients can be performed in a very efficient manner. The expansion can be separately performed for the angular part using a spherical harmonic transformation and for the radial part using an ordinary 1D Fourier transformation. Fast algorithms exist for both transformations [4, 8]. A brief sketch of the fast computation of expansion coefficients \mathbf{a}_ℓ^{Rk} with $a_{\ell m}^{Rk} := \langle f, E_{\ell m}^{Rk} \rangle$ is given in the following:

$$\begin{aligned} \langle f, E_{\ell m}^{Rk} \rangle &= \\ &= \int_0^R \int_0^\pi \int_0^{2\pi} f(r, \theta, \phi) \overline{E_{\ell m}^{Rk}(r, \theta, \phi)} r^2 d\Omega dr \\ &= \iiint f(r, \theta, \phi) \overline{Y_m^\ell(\theta, \phi)} w_{-k}^R(r) r d\Omega dr \end{aligned} \quad (16)$$

Weighting each voxel by its distance to the object centre $f'(r, \theta, \phi) = r f(r, \theta, \phi)$ leads to:

$$\begin{aligned} \langle f, E_{\ell m}^{Rk} \rangle &= \dots \\ &= \iiint f'(r, \theta, \phi) \overline{Y_m^\ell(\theta, \phi)} w_{-k}^R(r) d\Omega dr \\ &= \int w_{-k}^R(r) \underbrace{\iiint f'(r, \theta, \phi) \overline{Y_m^\ell(\theta, \phi)} d\Omega}_{b_{\ell m}(r)} dr \end{aligned} \quad (17)$$

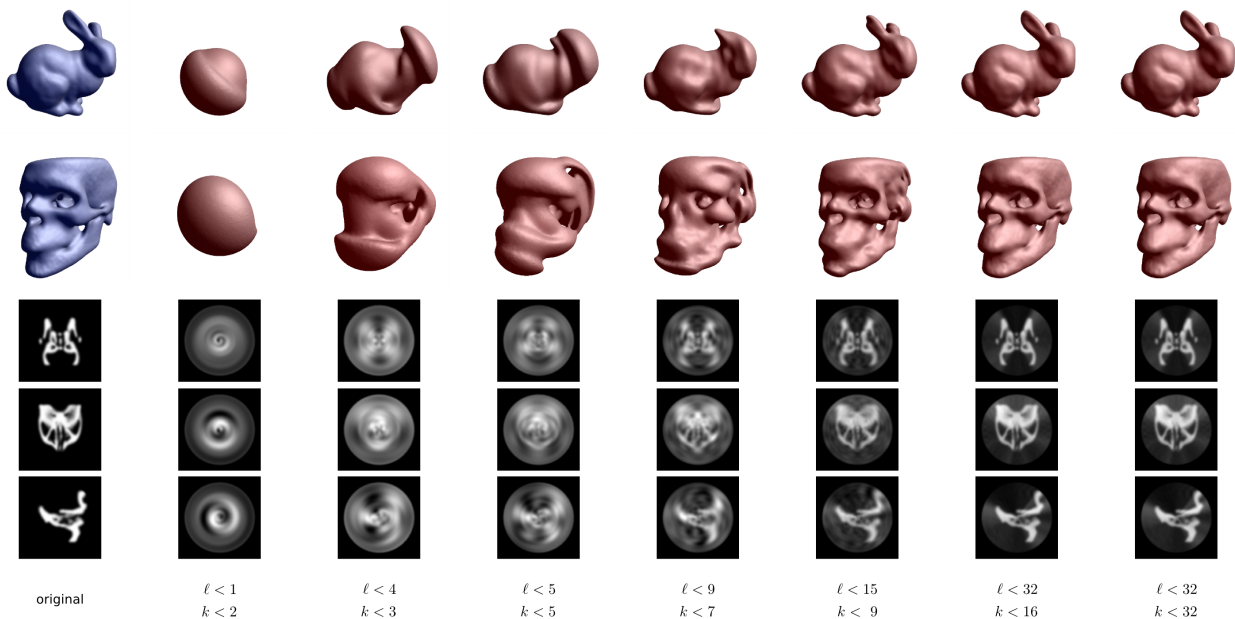


Figure 2. Reconstruction of models of the Princeton Shape Benchmark presented in a spherical voxel grid ($173_r \times 256_\theta \times 256_\phi$) corresponding to 11337728 voxel. A voxel based volume rendering shows a rabbit and a skull. The skull is shown together with the corresponding Z/Y/X planes intersecting with the origin of the ball. For $\ell = 32, k = 16$ we have only 9248 spherical Fourier harmonics coefficients sufficiently describing the volumetric object, leading to an 1632-dimensional descriptor.

The radius dependent angular expansion coefficient $b_{\ell m}(r)$ is obtained by a spherical harmonics transformation. The final expression can then be evaluated by a 1D Fourier transformation:

$$\begin{aligned}
 \langle f, E_{\ell m}^{Rk} \rangle &= \dots \\
 &= \int_0^R w_{-k}^R(r) b_{\ell m}(r) dr \\
 &= a_{\ell m}^{Rk}
 \end{aligned} \tag{18}$$

3.2. Rotational Behaviour

The rotational behaviour of the expansion coefficients \mathbf{a}_ℓ^{Rk} can be directly derived from the rotation property of the spherical harmonics expansion coefficients (eq. (7)). Given a rotation $g \in SO(3)$ acting on a function on the closed ball, the spherical harmonics expansion coefficient $\mathbf{b}_\ell(r)$ transform with respect to the Wigner D-Matrix \mathbf{D}_g^ℓ to $\mathbf{b}'_\ell(r) = \mathbf{D}_g^\ell \mathbf{b}_\ell(r)$. Expressing \mathbf{D}_g^ℓ in row vectors \mathbf{d}_m^ℓ :

$$\mathbf{D}_g^\ell = \underbrace{\begin{pmatrix} d_{-\ell, -\ell} & \dots & d_{-\ell \ell} \\ \vdots & \ddots & \vdots \\ d_{00} & \dots & d_{0\ell} \\ \vdots & \ddots & \vdots \\ d_{\ell, -\ell} & \dots & d_{\ell \ell} \end{pmatrix}}_{(2\ell+1) \times (2\ell+1)} = \begin{pmatrix} \mathbf{d}_{-\ell}^\ell \\ \vdots \\ \mathbf{d}_0^\ell \\ \vdots \\ \mathbf{d}_\ell^\ell \end{pmatrix} \tag{19}$$

we have

$$\begin{aligned}
 b'_m{}^\ell &= (\mathbf{d}_m^\ell)^T \mathbf{b}_\ell \\
 &= d_{m, -\ell}^\ell b_{\ell, -\ell} + \dots + d_{m, 0}^\ell b_{\ell, 0} + \dots + d_{m, \ell}^\ell b_{\ell, \ell}
 \end{aligned} \tag{20}$$

We can then easily show that the expansion coefficients \mathbf{a}_ℓ^{Rk} transform with respect to \mathbf{D}_g^ℓ , too:

$$\begin{aligned}
 a_{\ell m}^{\prime Rk} &= \\
 &= \int_0^R w_{-k}^R(r) b'_{\ell m}(r) dr \\
 &= (\mathbf{d}_m^\ell)^T \begin{pmatrix} \int_0^R w_{-k}^R(r) b_{\ell, -\ell}(r) dr \\ \vdots \\ \int_0^R w_{-k}^R(r) b_{\ell, \ell}(r) dr \end{pmatrix} \\
 &= (\mathbf{d}_m^\ell)^T \mathbf{a}_\ell^{Rk}
 \end{aligned} \tag{21}$$

It follows, that $\mathbf{a}_\ell^{\prime Rk} = \mathbf{D}_g^\ell \mathbf{a}_\ell^{Rk}$.

3.3. Spherical Fourier Harmonic Descriptors

For the design of descriptors relying on the idea of group integration [15] we use of the tensor product (eq. (10)) as an extension to the ordinary scalar product used in [6, 17]. For each expansion coefficient \mathbf{a}_ℓ^{Rk} , we get a three-dimensional

feature vector $\mathbf{c}_\ell^{Rk} \in \mathbb{R}_+^3$, where:

$$c_{\ell 0}^{Rk} = |\text{Real}((\mathbf{a}_\ell^{Rk} \bullet_0 \mathbf{a}_\ell^{Rk})^{\frac{1}{2}})| \quad (22)$$

$$c_{\ell 1}^{Rk} = |\text{Imag}((\mathbf{a}_\ell^{Rk} \bullet_0 \mathbf{a}_\ell^{Rk})^{\frac{1}{2}})| \quad (23)$$

$$\begin{aligned} c_{\ell 2}^{Rk} &= (\mathbf{a}_\ell^{Rk} \bullet_0 \mathbf{a}_\ell^{R,-k})^{\frac{1}{2}} = \langle \mathbf{a}_\ell^{Rk}, \mathbf{a}_\ell^{Rk} \rangle^{\frac{1}{2}} \\ &= \|\mathbf{a}_\ell^{Rk}\| \end{aligned} \quad (24)$$

The phase information of the coefficient is preserved in the components $c_{\ell 0}^{Rk}$ and $c_{\ell 1}^{Rk}$ while the computation of $c_{\ell 2}^{Rk}$ coincides with the ordinary scalar product (due to eq. (15)) representing the energy for certain bands ℓ and k . Our experiments have shown, that in all cases the combination of features preserving both, the phase information and the total energy perform much better (psb test set: 59%) than only using the phase preserving feature (psb test set: 56%) or only considering the energy (psb test set: 55.7%). The descriptor \mathbf{F}_{KL} representing the object in a rotation invariant way is formed by concatenating all feature vectors that can be derived for given bandwidth limits K and L for k and ℓ , respectively.

$$\mathbf{F}_{KL} = \{\mathbf{c}_0^{0T}, \dots, \mathbf{c}_\ell^{RkT}, \dots, \mathbf{c}_L^{RK^T}\} \quad (25)$$

for $0 \leq \ell \leq L$ and $0 \leq k \leq K$. In all our experiments we normalise the descriptors with respect to the $l1$ norm.

4. Experiments

We choose the Princeton Shape Benchmark (PSB) [16] for testing the performance of the spherical Fourier harmonic descriptors. The PSB provides 1814 triangulated models, divided into 161 classes. Each class consists of at least four models. The database is equally divided into a test and a training set. Tools are provided to obtain performance measurements on the test set and the training set that can easily be compared. For a description of the used performance measures Nearest-Neighbour/1st-Tier/2nd-Tier/E-Measure/Discounted-Cumulative-Gain see [16]. For our experiments we present the models into a 200^3 voxel grid and align them with respect to their centre of mass. The volume is smoothed by an isotropic gaussian kernel with $\sigma = 4.5$. The software we are using [8, 4] requires a representation in spherical coordinates according to eq. (3). We choose a one-voxel-spaced radial sampling and a sampling in 64 steps for the longitude θ and the colatitude ϕ . The final image dimension is $173_r \times 64_\theta \times 64_\phi$.

We compare the ordinary spherical harmonic descriptor (SHD) to our spherical Fourier harmonic descriptor (SFHD) extracted from intensity values. The expansion of the angular part is the same for an expansion in spherical harmonics and for a spherical Fourier harmonics expansion. Hence the descriptors only differ in the way how they represent the radial component. The SHD are based on a spherical

harmonics expansion of independent nested spheres which results in descriptors describing each sphere independently. In contrast, the SFHD do explicitly represent the relation of the angular part in radial direction. This induces the questions of the importance of the radial relation considered in our SFHD.

First we try to reproduce the results published in [16] which were obtained using the SHD (Nearest neighbour LOOCV¹ on the test set using the SHD: 55.6%). We vary the step size of radial sampling between 1 and 10 voxel and evaluate the performance for different bandwidth limits between 4 and 32. We obtain the best results measured by the tools provided in [16] by using a radial sampling in 7 voxel steps resulting in 25 spheres, weighting each sphere by the squared radius and doing a spherical harmonic expansion up to the 25th band. With this setting we get 55% in the LOOCV task using the test set. For all results (Nearest-Neighbour/1st-Tier/2nd-Tier/E-Measure/Discounted-Cumulative-Gain) that we get on the test set and training set see the second row of table 1 and table 2.

We secondly conduct experiments measuring the performance of the SFHD. We vary the bandwidth limit of the spherical harmonic expansion to values between 4 and 32. The radial band limit is also varied between 4 and 32. The best results (first row of table 1 and table 2) are obtained for the highest bandwidth, namely 32 for the radial part and 32 for the angular part, respectively.

In figure 4 we show the performance of the SHD compared to our SFHD for varying bandwidth of the spherical harmonics expansion. The bandwidth limit for the radial transformation is constantly set to 32. A LOOCV considering all 1814 models additionally emphasizes the superiority of the SFHD over the SHD. Only for lower bandwidth (< 8) the SHD perform better. A similar behaviour has already been observed for the Bessel functions [17]. Figure 5 shows the performance for different bandwidth limits of the radial transformation. We can observe, that a small set of 16 basis functions is sufficient to get satisfactory results, which means we can drastically reduce the size of a descriptor without loosing the ability of object discrimination. This observation corresponds to the visual appearance of the reconstructed models for $\ell < 32, k < 16$ depicted in figure 2.

Table 1. Results based on the PSB test-set (907 objects) comparing the SHD descriptors to the SFHD

Method	NN	1stT	2ndT	EM	DCG
SFHD	59.0 %	30.1 %	40.0%	23.5%	57.5%
SHD	55.0%	28.6%	38.2%	22.7%	55.8%

¹leave one out cross validation



Figure 3. Some models of the Princeton Shape Benchmark presented in a 200^3 voxel grid.

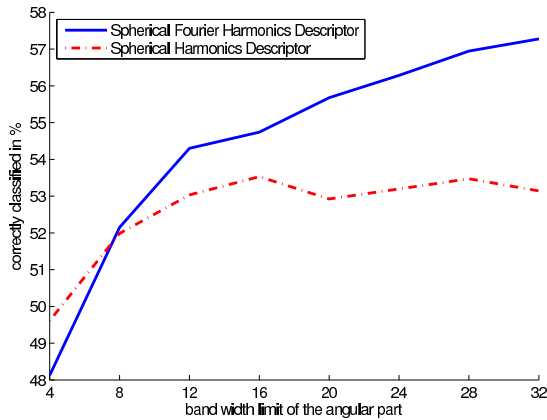


Figure 4. Performance of the spherical Fourier harmonic descriptor and the spherical harmonic descriptor for different band limits of the angular part. For comparison purpose we perform a LOOCV using all 1814 models (divided into 161 classes) of the PSB.

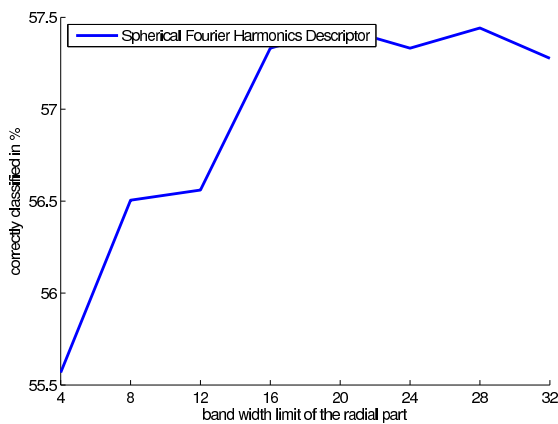


Figure 5. Performance of the spherical Fourier harmonic descriptor for varying radial bandwidth limits using all 1814 models. The bandwidth for the angular part is constantly set to 32.

Table 2. Results based on the PSB training-set (907 objects) comparing the SHD descriptors to the SFHD

Method	NN	1stT	2ndT	EM	DCG
SFHD	59.2 %	32.5 %	43.6 %	23.8%	60.2%
SHD	56.9%	30.1%	40.7%	22.7 %	57.9%

5. Conclusion

We present a novel approach deriving rotation invariant descriptors from three-dimensional objects. Our approach extends the widely used spherical harmonic descriptors and therefore inherits all the gentle properties known from the spherical harmonics theory and the Fourier theory. More precisely, we directly benefit from fast and efficient algorithms available for the angular transformation (spherical harmonics transformation) and for the radial transformation (1D Fourier transformation) and can derive a rotation invariant object representation in an analytical way. We further propose the usage of a tensor product for deriving the rotation invariant representation of descriptors preserving the phase information of the expansion coefficients. We conducted experiments comparing the spherical harmonic descriptors to our spherical Fourier harmonic descriptors. Our experiments have proven the superiority of the spherical Fourier harmonic descriptors since the performance notably increases when taking the radial transformation into account. For future work we plan an extensive study comparing the performance of descriptors based on different kinds of radial basis functions. We also plan to consider further object databases containing biological image data or images obtained from robot controlled laser scanning devices.

Acknowledgement

This study was supported by the Excellence Initiative of the German Federal and State Governments (EXC 294)

References

- [1] D. M. Brink and G. Satchler. *Angular Momentum*. Oxford Science Publications, 1993.
- [2] N. Canterakis. 3D zernike moments and zernike affine invariants for 3D image analysis and recognition. In *11th Scandinavian Conf. on Image Analysis*, Kangerlussuaq, Greenland, 1999.
- [3] J. Fang and G. Qiu. Human face detection using angular radial transform and support vector machines. In *Proceedings of the International Conference on Image Processing 2003*, volume 1, pages I-669-72 vol.1, Sept. 2003.
- [4] M. Frigo and S. G. Johnson. The design and implementation of FFTW3. *Proceedings of the IEEE*, 93(2):216-231, 2005. Special issue on "Program Generation, Optimization, and Platform Adaptation".

- [5] R. Green. Spherical harmonic lighting: The gritty details. *Archives of the Game Developers Conference*, March 2003.
- [6] M. Kazhdan, T. Funkhouser, and S. Rusinkiewicz. Rotation invariant spherical harmonic representation of 3D shape descriptors. In *Symposium on Geometry Processing*, June 2003.
- [7] J. Koenderink and A. van Doorn. Generic neighborhood operators. *Pattern Analysis and Machine Intelligence, IEEE Transactions on*, 14(6):597–605, Jun 1992.
- [8] P. J. Kostelec and D. N. Rockmore. S2kit: A lite version of sphermonickit. Department of Mathematics. Dartmouth College, 2004.
- [9] M. Reisert. *Group Integration Techniques in Pattern Analysis - A Kernel View*. PhD thesis, Albert-Ludwigs-Universität Freiburg, 2008.
- [10] M. Reisert and H. Burkhardt. Second order 3d shape features: An exhaustive study. *C&G, Special Issue on Shape Reasoning and Understanding*, 30(2), 2006.
- [11] M. Reisert and H. Burkhardt. Efficient tensor voting with 3d tensorial harmonics. In *Computer Vision and Pattern Recognition Workshops, 2008. CVPRW '08. IEEE Computer Society Conference on*, pages 1–7, 2008.
- [12] J. Ricard, D. Coeurjolly, and A. Baskurt. Generalizations of angular radial transform for 2d and 3d shape retrieval. *Pattern Recognition Letters*, 26(14):2174–2186, October 2005.
- [13] O. Ronneberger, Q. Wang, and H. Burkhardt. 3d invariants with high robustness to local deformations for automated pollen recognition. In *Proceedings of the DAGM 2007*, pages 455–435, Heidelberg, Germany, 2007. LNCS, Springer.
- [14] M. Rose. *Elementary Theory of Angular Momentum*. Dover Publications, 1995.
- [15] H. Schulz-Mirbach. *Anwendung von Invarianzprinzipien zur Merkmalgewinnung in der Mustererkennung*. PhD thesis, Technische Universität Hamburg-Harburg, 1995. Reihe 10, Nr. 372, VDI-Verlag.
- [16] P. Shilane, P. Min, M. Kazhdan, and T. Funkhouser. The princeton shape benchmark. In *Shape Modeling and Applications*, pages 167–178, 2004.
- [17] Q. Wang, O. Ronneberger, and H. Burkhardt. Rotational invariance based on fourier analysis in polar and spherical coordinates. *IEEE Transactions on Pattern Analysis and Machine Intelligence*, 2009. accepted.